A HYSTERETIC FORMULATION FOR ISOGEOMETRIC ANALYSIS AND SHAPE OPTIMIZATION OF PLANE STRESS STRUCTURES

A. N. Moysidis, V. K. Koumousis

Institute of Structural Analysis & Aseismic Research
National Technical University of Athens
Zografou Campus, 15780, Athens, Greece
e-mail: argi_n_m@hotmail.com ; vkoum@central.ntua.gr

Keywords: Hysteretic Finite Elements, Bouc-Wen Model, Isogeometric Analysis, Shape Optimization.

Abstract. *In this work, a new hysteretic formulation for the inelastic static and dynamic analysis of plane stress problems within the framework of Isogeometric Analysis (IGA) is presented. The Bouc-Wen model is utilized as a smooth hysteretic, rate independent model, capable of expressing the hysteretic behaviour that can be easily extended to account for stiffness degradation, strength deterioration and pinching phenomena. On the basis of the classical theory of plasticity, the generalized 3D Bouc-Wen model is expressed in tensorial form incorporating the yield criterion and linear or nonlinear, isotropic or kinematic hardening law. Subsequently, basis functions generated from Non-Uniform Rational B-Splines (NURBS) and the appropriate control points define the structure's geometry and are employed to build the elastic stiffness matrix. Then, the elastic formulation is extended by considering as additional hysteretic degrees of freedom the plastic strains at the quadrature points defined by the appropriate quadrature rule for the numerical integration. The evolution of the plastic strains is determined by a Bouc–Wen evolution equation and the solution provides the displacements at control points of the structure and the plastic strains at the quadrature points. On the basis of the proposed formulation the shape optimization problem is formulated using mathematical programming. The objective function is the minimum mass of the structure and the control points of the boundary and/or the control weights are selected as the optimization design variables. Furthermore, stress and displacement constraints are imposed at specific points. Finally, numerical results are presented that validate the proposed hysteretic formulation. A good agreement is achieved between the standard FEM and the proposed scheme.*

1 INTRODUCTION

Isogeometric analysis (IGA) is an energy based computational method for the solution of boundary value problems. The main concept of the IGA is that the same functions (B-splines and NURBS) used in Computer Aided Design (CAD) to handle the graphics are also used to interpolate the geometry and the displacement field. One of the advantages of IGA relies on the fact that IGA offers greater precision and interaction between the overall modeling and analysis process, whereas the finite element mesh is only an approximation of the "exact" CAD geometry. Moreover, the benefits of shape optimization using IGA are very important because geometry and meshing are tightly connected and the geometry-to-mesh mapping is automatic. In this work, the Bouc-Wen model is utilized as a smooth hysteretic, rate independent model, capable of expressing the hysteretic behavior and it is incorporated in an IGA code. In this respect, the elastic formulation is extended by considering as additional hysteretic degrees of freedom the plastic strains at the quadrature points defined by the appropriate quadrature rule for the numerical integration. The evolution of the plastic strains is determined by a Bouc–Wen evolution equation. In this way, the elastic and hysteretic stiffness matrices of the structure are derived and are assembled to form the equations of motion. The evolution equations for the hysteretic degrees of freedom constitute an additional set of first order nonlinear equations which together with the equations of motion determine the system of equations that describes the inelastic problem. The entire system of equations is converted into state space form and the solution is established on the basis of a Livermore integration scheme. Numerical results are presented that justify the validity and accuracy of the proposed formulation. Moreover, a shape optimization problem is formulated using mathematical programming based on NURBS geometries.

2 B-SPLINES AND NURBS GEOMETRIES

Let $\Xi = \left\{\xi_1,\ldots,\xi_{n+p+1}\right\}$ be a non-decreasing sequence of real numbers, i.e. $\xi_i \le \xi_{i+1}$, $i = 1,\ldots,n+p$. The ξ_i are called knots and Ξ is the knot vector [1]. The i^{th} B-spline basis function of p-degree, denoted by $N_{i,p}(\xi)$, is defined recursively as:

$$N_{i,0}(\xi)=\begin{cases}1 & if\ \xi_i \le \xi \le \xi_{i+1}\\ 0 & otherwise\end{cases}$$
$$N_{i,p}(\xi)=\frac{\xi-\xi_i}{\xi_{i+p}-\xi_i}N_{i,p-1}(\xi)+\frac{u_{i+p+1}-\xi}{\xi_{i+p+1}-\xi_{i+1}}N_{i+1,p-1}(\xi) \tag{1}$$

If $n+p+1$ is the number of knots, there exist n basis functions. The half-open interval $[\xi_i,\xi_{i+1})$ is called the i^{th} knot span. The knot vectors which have the form:

$$\Xi=\left\{\underbrace{a,\ldots a}_{p+1},\xi_{p+2},\ldots,\xi_n,\underbrace{b,\ldots b}_{p+1}\right\} \tag{2}$$

that is the first and last knot has multiplicity $p+1$, are defined as non-periodic or open. Moreover, a knot vector is uniform if all interior knots are equally spaced. Otherwise it is non-uniform. The derivative of a basis function is given by:

$$N'_{i,p}=\frac{p}{\xi_{i+p}-\xi_i}N_{i,p-1}(\xi)-\frac{p}{\xi_{i+p+1}-\xi_{i+1}}N_{i+1,p-1}(\xi) \tag{3}$$

A pth degree B-spline curve is defined by:

$$\mathbf{C}(\xi)=\sum_{i=1}^{n}N_{i,p}(\xi)\mathbf{P}_i \qquad a\le\xi\le b \tag{4}$$

where $\{\mathbf{P}_i\}$ are the control points and $N_{i,p}(\xi)$ are the p^{th} degree B-spline basis functions defined on the non-periodic knot vector of Eq. (2). The $\{\mathbf{P}_i\}$ are the vertices of the control polygon. The derivative of a B-spline curve is given by the expression:

$$\mathbf{C}'(\xi)=\sum_{i=1}^{n}N'_{i,p}(\xi)\mathbf{P}_i \tag{5}$$

An example is presented in Figure 1 for polynomial order $p=3$ and the open, non-uniform knot vector $\Xi=\{0,0,0,0,1,1,2,3,3,3,4,5,5,5,5\}$. The control polygon is $\{\mathbf{P}_i\}=\left[\begin{pmatrix}0\\-2\end{pmatrix},\begin{pmatrix}-4\\1\end{pmatrix},\begin{pmatrix}-4\\3\end{pmatrix},\begin{pmatrix}-3\\4\end{pmatrix},\begin{pmatrix}-1\\2\end{pmatrix},\begin{pmatrix}2\\8\end{pmatrix},\begin{pmatrix}5\\7\end{pmatrix},\begin{pmatrix}2\\4\end{pmatrix},\begin{pmatrix}7\\2\end{pmatrix},\begin{pmatrix}8\\0\end{pmatrix},\begin{pmatrix}6\\-1\end{pmatrix}\right]$.

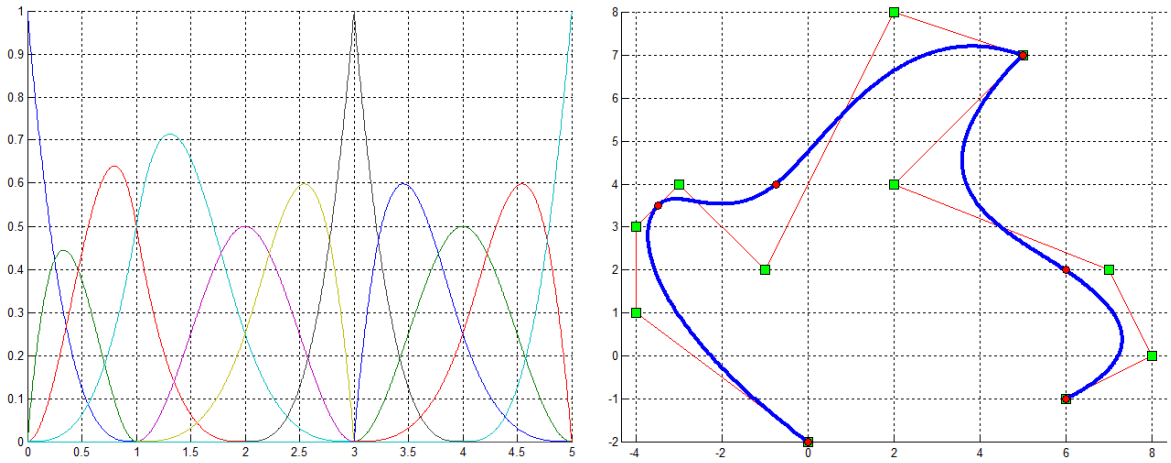

Figure 1.(a) Basis functions, (b) B-spline curve (control points( ), knot locations( ))

A tensor product B-spline surface is defined by the relation:

$$\mathbf{S}(\xi,\eta)=\sum_{i=1}^{n}\sum_{j=1}^{m}N_{i,p}(\xi)N_{j,q}(\eta)\mathbf{P}_{i,j} \qquad \xi_1\le\xi\le\xi_{n+p+1},\ \eta_1\le\eta\le\eta_{m+q+1} \tag{6}$$

where $\{\mathbf{P}_{i,j}\}$ is the control net, $N_{i,p}(\xi)$ are the p^{th} degree B-spline basis functions defined on the non-periodic knot vector $\Xi=\{\xi_1,\ldots,\xi_{n+p+1}\}$ and $N_{j,q}(\eta)$ are the q^{th} degree B-spline basis functions defined on the non-periodic knot vector $\mathrm{H}=\{\eta_1,\ldots,\eta_{m+q+1}\}$.

Coming to the Non Uniform Rational B-Spline (NURBS) curves, conic sections and circles are widely used in computer graphics and computer aided design. One of the greatest advantages of NURBS is their capability of precisely representing conic sections and circles in contrast to non-rational B-splines. A p^{th} degree NURBS curve is given by:

$$\mathbf{C}(\xi)=\frac{\sum_{i=1}^{n}N_{i,p}(\xi)w_i\mathbf{P}_i}{\sum_{i=1}^{n}N_{i,p}(\xi)w_i}=\frac{\mathbf{A}(\xi)}{w(\xi)} \qquad a\le\xi\le b \tag{7}$$

where $\{\mathbf{P}_i\}=\{(x_i,y_i,z_i)\}$ are the control points (forming a control polygon), $\{w_i\}$ are the weights and $N_{i,p}(\xi)$ are the p^{th} degree B-spline basis functions defined on the non-periodic knot vector of Eq. (2). It is usually assumed that $a=0$, $b=0$ and $w_i>0$ for all i. From the geometric point of view, a NURBS curve is the projection of a non-rational (polynomial) B-spline curve defined in four-dimensional (4D) homogeneous coordinate space back into three-dimensional (3D) physical space. The non-rational B-spline in four-dimensional space is defined by the relation:

$$\mathbf{C}^w(\xi)=\sum_{i=1}^{n}N_{i,p}(\xi)\mathbf{P}_i^w \tag{8}$$

where $\mathbf{P}_i^w=(w_ix_i,w_iy_i,w_iz_i,w_i)$ are the weighted control points. The derivative of a NURBS curve is evaluated by:

$$\mathbf{C}'(\xi)=\frac{w(\xi)\mathbf{A}'(\xi)-w'(\xi)\mathbf{A}(\xi)}{(w(\xi))^2}=\frac{\mathbf{A}'(\xi)-w'(\xi)\mathbf{C}(\xi)}{w(\xi)} \tag{9}$$

where the derivatives of $\mathbf{A}(\xi)$ and $w(\xi)$ are computed by the Eq. (5).

A NURBS surface of degree p in the ξ direction and degree q in η direction is defined by:

$$\mathbf{S}(\xi,\eta)=\frac{\sum_{i=1}^{n}\sum_{j=1}^{m}N_{i,p}(\xi)N_{j,q}(\eta)w_{i,j}\mathbf{P}_{i,j}}{\sum_{i=1}^{n}\sum_{j=1}^{m}N_{i,p}(\xi)N_{j,q}(\eta)w_{i,j}} \qquad \xi_1\le\xi\le\xi_{n+p+1},\ \eta_1\le\eta\le\eta_{m+q+1} \tag{10}$$

where $\{\mathbf{P}_{i,j}\}=\{(x_{i,j},y_{i,j},z_{i,j})\}$ are the control points (forming a bidirectional control net), $\{w_{i,j}\}$ are the weights, $N_{i,p}(\xi)$ are the p^{th} degree B-spline basis functions defined on the non-periodic knot vector $\Xi=\{\xi_1,\ldots,\xi_{n+p+1}\}$ and $N_{j,q}(\eta)$ are the q^{th} degree B-spline basis functions defined on the non-periodic knot vector $\mathrm{H}=\{\eta_1,\ldots,\eta_{m+q+1}\}$. Alternatively, a NURBS surface can be represented using homogeneous coordinates as:

$$\mathbf{S}^w(\xi,\eta)=\sum_{i=1}^{n}\sum_{j=1}^{m}N_{i,p}(\xi)N_{j,q}(\eta)\mathbf{P}_{i,j}^w \tag{11}$$

where $\mathbf{P}_{i,j}^w=(w_{i,j}x_{i,j},w_{i,j}y_{i,j},w_{i,j}z_{i,j},w_{i,j})$.

3 ISOGEOMETRIC ANALYSIS AND SHAPE OPTIMIZATION

Isogeometric analysis extends the isoparametric concept offering better abilities to handle the graphics [2]. Thus, the solution space and the geometry are interpolated using the same scheme. The main difference between FEA and IGA is that in classical FEA an interpolation scheme is selected for the displacement field and the same scheme is used to approximate the geometry. On the contrary, in IGA the appropriate B-spline/NURBS basis, which exactly describes and handles modifications of the geometry, is used to approximate the unknown solution field. Especially, in the case of plane stress problems, the solution-displacement field is defined as:

$$\left\{u(\xi,\eta)\right\}=\begin{Bmatrix}u_x(\xi,\eta)\\ u_y(\xi,\eta)\end{Bmatrix}=\frac{\sum_{i=1}^{n}\sum_{j=1}^{m}N_{i,p}(\xi)N_{j,q}(\eta)w_{i,j}\begin{Bmatrix}d_x\\ d_y\end{Bmatrix}_{i,j}}{\sum_{i=1}^{n}\sum_{j=1}^{m}N_{i,p}(\xi)N_{j,q}(\eta)w_{i,j}}=\sum_{i=1}^{n}\sum_{j=1}^{m}R_{i,j}(\xi,\eta)\left\{d\right\}_{i,j} \tag{12}$$

where $R_{i,j}(\xi,\eta)=\left[N_{i,p}(\xi)N_{j,q}(\eta)w_{i,j}\right]\Big/\left[\sum_{i=1}^{n}\sum_{j=1}^{m}N_{i,p}(\xi)N_{j,q}(\eta)w_{i,j}\right]$ and $\left\{d\right\}_{i,j}$ are the control variables, i.e. the value of displacement at the control point (i,j). It is very convenient to determine a scheme for the global numbering of basis functions such that:

$$A=n(j-1)+i \tag{13}$$

and

$$\tilde{N}_A(\xi,\eta)=R_{i,j}(\xi,\eta) \tag{14}$$

By means of Eq. (14) the displacement field of Eq. (12) can be stated in the following form:

$$\left\{u(\xi,\eta)\right\}=\sum_{A=1}^{n\times m}\tilde{N}_A(\xi,\eta)\left\{d_A\right\} \tag{15}$$

The infinitesimal strain vector (plane stress conditions) is defined by the following relation:

$$\left\{\varepsilon\right\}=\begin{Bmatrix}\varepsilon_{xx}\\ \varepsilon_{yy}\\ \gamma_{xy}\end{Bmatrix}=\begin{Bmatrix}\partial u_x/\partial x\\ \partial u_y/\partial y\\ \partial u_x/\partial y+\partial u_y/\partial x\end{Bmatrix}=\sum_{A=1}^{n\times m}\begin{bmatrix}\tilde{N}_{A,1}(\xi,\eta) & 0\\ 0 & \tilde{N}_{A,2}(\xi,\eta)\\ \tilde{N}_{A,2}(\xi,\eta) & \tilde{N}_{A,1}(\xi,\eta)\end{bmatrix}\begin{Bmatrix}d_x\\ d_y\end{Bmatrix}_A=\sum_{A=1}^{n\times m}\left[B_A\right]\left\{d_A\right\}=\left[B\right]\left\{d\right\} \tag{16}$$

where $\left\{d\right\}=\left\{\left\{d_x,d_y\right\}_1,\ldots,\left\{d_x,d_y\right\}_{(n\times m)}\right\}^T$ is the vector of the unknown control variables. For an isotropic material, one can write:

$$\left\{\sigma\right\}=\begin{Bmatrix}\sigma_{xx}\\ \sigma_{yy}\\ \tau_{xy}\end{Bmatrix}=\frac{E}{1-\nu^2}\begin{bmatrix}1 & \nu & 0\\ \nu & 1 & 0\\ 0 & 0 & \dfrac{1-\nu}{2}\end{bmatrix}\begin{Bmatrix}\varepsilon_{xx}\\ \varepsilon_{yy}\\ \gamma_{xy}\end{Bmatrix}=\left[C\right]\begin{Bmatrix}\varepsilon_{xx}\\ \varepsilon_{yy}\\ \gamma_{xy}\end{Bmatrix} \tag{17}$$

The expression for the principle of virtual work in this case is written as:

$$
\begin{gathered}
W_{\text{int}} = W_{ext} \Leftrightarrow \int_{\Omega} \{\bar{\varepsilon}\}^{\mathrm{T}} \{\sigma\} d\Omega = \{\bar{d}\}^{T} \{R\} \Leftrightarrow \\
\int_{\xi_1}^{\xi_{n+p+1}} \int_{\eta_1}^{\eta_{m+q+1}} \{\bar{\varepsilon}\}^{\mathrm{T}} [C] \{\varepsilon\} t \det[J] d\eta d\xi = \{\bar{d}\}^{T} \{R\} \Leftrightarrow \\
\{\bar{d}\} \int_{\xi_1}^{\xi_{n+p+1}} \int_{\eta_1}^{\eta_{m+q+1}} [B]^{\mathrm{T}} [C][B] \{d\} t \det[J] d\eta d\xi = \{\bar{d}\}^{T} \{R\} \Leftrightarrow \\
\int_{\xi_1}^{\xi_{n+p+1}} \int_{\eta_1}^{\eta_{m+q+1}} [B]^{\mathrm{T}} [C][B] \{d\} t \det[J] d\eta d\xi = \{R\}
\end{gathered}
\tag{18}
$$

where $\{\bar{d}\}$ are the virtual displacements, $\{\bar{\varepsilon}\}$ are the corresponding virtual strains and $[J] = \begin{bmatrix} \partial x/\partial \xi & \partial y/\partial \xi \\ \partial x/\partial \eta & \partial y/\partial \eta \end{bmatrix}$ is the Jacobian matrix. The last of integrals of Eq. (18) is evaluated numerically by applying an appropriate quadrature rule.

4 INELASTIC BEHAVIOR AND BOUC – WEN HYSTERETIC MODEL

The response of most materials when stressed up to certain level, remains elastic. In this range they exhibit no memory on their reached stress-strain state and return to zero stress – strain when unloaded. In stress space, the elastic domain is delimited by an external boundary, i.e. the yield surface, which is defined by a yield function of the form:

$$\Phi\left(\sigma_{ij}, \sigma_y^0\right) = f\left(\sigma_{ij}\right) - \sigma_y^0 = 0 \tag{19}$$

where σ_y^0 is the initial yield stress, whereas any admissible stress state must satisfy the condition $\Phi\left(\sigma_{ij}, \sigma_y^0\right) \le 0$. Loading further the material, plastic yielding or plastic flow, manifested as permanent strains at unloading. This is described by the plastic flow rule:

$$\underset{(\text{tensor components notation})}{\dot{\varepsilon}_{ij}^{pl} = \dot{\lambda} \frac{\partial Q\left(\sigma_{ij}\right)}{\partial \sigma_{ij}}} \quad or \quad \underset{(\text{tensor notation})}{\dot{\boldsymbol{\varepsilon}}^{pl} = \dot{\lambda} \frac{\partial Q(\boldsymbol{\sigma})}{\partial \boldsymbol{\sigma}}} \quad or \quad \underset{(\text{matrix-vector notation})}{\left\{\dot{\varepsilon}^{pl}\right\} = \dot{\lambda} \frac{\partial Q\left(\{\sigma\}\right)}{\partial \{\sigma\}}} \tag{20}$$

where $Q\left(\sigma_{ij}\right)$ is a plastic potential function and $\dot{\lambda}$ is the plastic multiplier. For most civil engineering materials, not including soils, a common valid approach is to associate the plastic potential with the yield function, $Q\left(\sigma_{ij}\right) = \Phi\left(\sigma_{ij}\right)$ (associated flow rule) and express eq. (20) as:

$$\dot{\varepsilon}_{ij}^{pl} = \dot{\lambda} \frac{\partial \Phi\left(\sigma_{ij}\right)}{\partial \sigma_{ij}} \qquad or \qquad \dot{\boldsymbol{\varepsilon}}^{pl} = \dot{\lambda} \frac{\partial \Phi(\boldsymbol{\sigma})}{\partial \boldsymbol{\sigma}} \tag{21}$$

Together with the evolution of the plastic strain, an evolution of the yield stress itself is also manifested (hardening) and the yield surface undergoes expansion and/or translation.

In the case of kinematic hardening, which is capable of predicting the Bauschinger effect, the yield function is expressed in the form:

$$\Phi = \Phi\left(\sigma_{ij}, \sigma_y^0\right) = f\left(\sigma_{ij} - \alpha_{ij}\right) - \sigma_y^0 = 0 \tag{22}$$

where $\boldsymbol{\alpha}$ is a tensorial back stress hardening parameter, that represents the evolution of the centre of the yield surface in the stress space. The back stress evolves as a function of the plastic multiplier, $\dot{\lambda}$ and the hardening function $\mathbf{G}$ as:

$$\underset{(\text{tensor notation})}{\dot{\boldsymbol{\alpha}} = \dot{\lambda} \mathbf{G}} \qquad or \qquad \underset{(\text{tensor components notation})}{\dot{\alpha}_{ij} = \dot{\lambda}\, G_{ij}} \qquad or \qquad \underset{(\text{matrix-vector notation})}{\{\dot{a}\} = \dot{\lambda} \{G\}} \tag{23}$$

In the case of Prager's linear kinematic hardening, evolution of the back stress is defined by the following linear relation:

$$\{\dot{\alpha}\} = C_p \{\dot{\varepsilon}^{pl}\} = C_p \left(\dot{\lambda} \frac{\partial \Phi}{\partial \{\sigma\}} \right) = \dot{\lambda} \{G\}, \qquad where \quad \{G\} = C_p \frac{\partial \Phi}{\partial \{\sigma\}} \tag{24}$$

where C_p is the hardening constant.

In addition the total strain tensor is considered as the sum of an elastic component ε_{ij}^{el} and a plastic component ε_{ij}^{pl} (assumption of additive decomposition) and thus:

$$\varepsilon_{ij} = \varepsilon_{ij}^{el} + \varepsilon_{ij}^{pl} \quad or \quad \boldsymbol{\varepsilon} = \boldsymbol{\varepsilon}^{el} + \boldsymbol{\varepsilon}^{pl} \tag{25}$$

Furthermore the stress increment is linearly related to the elastic strain increment in the plastic region and can be expressed by the following constitutive relation:

$$\begin{gathered} \dot{\sigma}_{ij} = C_{ijkl}\, \dot{\varepsilon}_{kl}^{el} = C_{ijkl} \left(\dot{\varepsilon}_{kl} - \dot{\varepsilon}_{kl}^{pl} \right) \quad or \quad \dot{\boldsymbol{\sigma}} = \mathbf{C} : \dot{\boldsymbol{\varepsilon}}^{el} = \mathbf{C} : \left(\dot{\boldsymbol{\varepsilon}} - \dot{\boldsymbol{\varepsilon}}^{pl} \right) \quad or \\ \{\dot{\sigma}\} = [C] \{\dot{\varepsilon}^{el}\} = [C] \left(\{\dot{\varepsilon}\} - \{\dot{\varepsilon}^{pl}\} \right) \end{gathered} \tag{26}$$

For plastic flow to occur, the stresses must remain on the yield surface (consistency condition) and hence:

$$\dot{\Phi} = \left\{ \frac{\partial \Phi}{\partial \{\sigma\}} \right\}^{\mathrm{T}} d\{\sigma\} + \left\{ \frac{\partial \Phi}{\partial \{\alpha\}} \right\}^{\mathrm{T}} d\{\alpha\} = 0 \quad or \quad \dot{\Phi} = \frac{\partial \Phi}{\partial \boldsymbol{\sigma}} : d\boldsymbol{\sigma} + \frac{\partial \Phi}{\partial \boldsymbol{\alpha}} : d\boldsymbol{\alpha} = 0 \tag{27}$$

In order to find $\dot{\lambda}$, eq. (26) is pre-multiplied by the flow vector $\left\{ \partial \Phi \big/ \partial \{\sigma\} \right\}^{\mathrm{T}}$ and using Eq. (27) and Eq. (21):

$$\dot{\lambda} = \left(- \left\{ \frac{\partial \Phi}{\partial \{\alpha\}} \right\}^{\mathrm{T}} \{G\} + \left\{ \frac{\partial \Phi}{\partial \{\sigma\}} \right\}^{\mathrm{T}} [C] \left\{ \frac{\partial \Phi}{\partial \{\sigma\}} \right\} \right)^{-1} \left\{ \frac{\partial \Phi}{\partial \{\sigma\}} \right\}^{\mathrm{T}} [C] \{\dot{\varepsilon}\} \tag{28}$$

Relation (28) holds only when yielding has occurred. Thus, by introducing the following Heaviside type functions:

$$H_1(\Phi) = \begin{cases} 1, & \Phi = 0 \\ 0, & \Phi < 0 \end{cases} \qquad H_2(\Phi) = \begin{cases} 1, & (\partial \Phi / \partial \boldsymbol{\sigma}) : d\boldsymbol{\sigma} \geq 0 \\ 0, & (\partial \Phi / \partial \boldsymbol{\sigma}) : d\boldsymbol{\sigma} < 0 \end{cases} \tag{29}$$

a single relation is established for the plastic multiplier in the whole stress space, which is the main intervention of the Bouc – Wen model ([3], [4]):

$$\dot{\lambda} = H_1 H_2 \left(- \left\{ \frac{\partial \Phi}{\partial \{\alpha\}} \right\}^{\mathrm{T}} \{G\} + \left\{ \frac{\partial \Phi}{\partial \{\sigma\}} \right\}^{\mathrm{T}} [C] \left\{ \frac{\partial \Phi}{\partial \{\sigma\}} \right\} \right)^{-1} \left\{ \frac{\partial \Phi}{\partial \{\sigma\}} \right\}^{\mathrm{T}} [C] \{\dot{\varepsilon}\} \tag{30}$$

To derive the Bouc-Wen relations, the two Heaviside functions are smoothened using the following expressions:

$$H_1 = \left| \frac{\Phi}{\Phi_0} \right|^N, \quad N \geq 2 \tag{31}$$

and (since there is no plastic deformation during unloading and $\dot{\lambda} = 0$):

$$H_2 = H\left(\left\{\frac{\partial\Phi}{\partial\{\sigma\}}\right\}^{\mathrm{T}}\{\dot{\sigma}\}\right) = \frac{1}{2}+\frac{1}{2}sign\left(\left\{\frac{\partial\Phi}{\partial\{\sigma\}}\right\}^{\mathrm{T}}[C]\{\dot{\varepsilon}\}\right) \tag{32}$$

Finally, using Eq. (21) and Eq. (30), the following Bouc – Wen model is derived:

$$\left\{\dot{\varepsilon}^{pl}\right\} = \underbrace{\left|\frac{\Phi}{\Phi_0}\right|^N}_{H_1}\underbrace{\left(\frac{1}{2}+\frac{1}{2}sign\left(\left\{\frac{\partial\Phi}{\partial\{\sigma\}}\right\}^{\mathrm{T}}[C]\{\dot{\varepsilon}\}\right)\right)}_{H_2}[R]\{\dot{\varepsilon}\} \tag{33}$$

where the interaction matrix $[R]$ is expressed as:

$$[R] = \left(-\left\{\frac{\partial\Phi}{\partial\{\alpha\}}\right\}^{\mathrm{T}}\{G\}+\left\{\frac{\partial\Phi}{\partial\{\sigma\}}\right\}^{\mathrm{T}}[C]\left\{\frac{\partial\Phi}{\partial\{\sigma\}}\right\}\right)^{-1}\left\{\frac{\partial\Phi}{\partial\{\sigma\}}\right\}\left\{\frac{\partial\Phi}{\partial\{\sigma\}}\right\}^{\mathrm{T}}[C] \tag{34}$$

and determines the necessary interrelations between the plastic strain components to secure that the stresses remain on the yield surface accounting also for the hardening law (consistency condition). In this rate form the Bouc-Wen model can incorporate any yield criterion and hardening law, encapsulating all different aspects of loading and unloading phases.

5 STIFFNESS AND HYSTERETIC MATRICES

The elastic deformation field is extended by introducing an additional matrix of hysteretic degrees of freedom which herein are the plastic strains at quadrature points:

$$[z] = \begin{bmatrix} \left\{\varepsilon^{pl}\right\}_{1,1} & \left\{\varepsilon^{pl}\right\}_{1,2} & \cdots & \left\{\varepsilon^{pl}\right\}_{1,mPl} \\ \left\{\varepsilon^{pl}\right\}_{2,1} & \left\{\varepsilon^{pl}\right\}_{2,2} & \cdots & \left\{\varepsilon^{pl}\right\}_{2,mPl} \\ \vdots & \vdots & \ddots & \vdots \\ \left\{\varepsilon^{pl}\right\}_{nPl,1} & \left\{\varepsilon^{pl}\right\}_{nPl,2} & \cdots & \left\{\varepsilon^{pl}\right\}_{nPl,mPl} \end{bmatrix} \tag{35}$$

where $\left\{\varepsilon^{pl}\right\}_{i,j}$ is the plastic component of the strain vector (16) at the (i,j) point of bidirectional net of quadrature points, where $i = 1,2,\ldots,n^p$, $j = 1,2,\ldots,m^p$ and $n^p \times m^p$ is the total number of quadrature points. At this point, a hysteretic tensor product B-spline surface – hysteretic field can be considered so that:

$$\left\{\varepsilon^{pl}\right\} = \sum_{i=1}^{n^p}\sum_{j=1}^{m^p} N^{pl}_{i,p^p}(\xi)\,N^{pl}_{j,q^p}(\eta)[z]_{i,j} = \sum_{A=1}^{n^p\times m^p}\tilde{N}^{pl}_A(\xi,\eta)\begin{Bmatrix}\varepsilon_{xx}\\ \varepsilon_{yy}\\ \gamma_{xy}\end{Bmatrix}_A = \sum_{A=1}^{n^p\times m^p}\tilde{N}^{pl}_A(\xi,\eta)\{z_A\} = \tilde{N}^{pl}\{z\} \tag{36}$$

where N^{pl}_{i,p^p} and N^{pl}_{j,q^p} are B-spline basis functions of preselected order p^p and q^p corresponding to knot vectors Ξ^{pl} and H^{pl} which are constructed in such a way that the hysteretic surface interpolating the plastic component of the strain vector of quadrature points doesn't result in erratic shapes (a more detailed presentation on the surface interpolation can be found in [1]). Moreover, $\{z\} = \left\{\{z\}_1^T,\ldots,\{z\}_{(n^p\times m^p)}^T\right\}^T$ is the vector of hysteretic degrees of freedom and $A = n^p(j-1)+i$.

The principle of virtual work (Eq. (18)), by means of relation (25), is expressed as:

$$\int_\Omega \{\bar{\varepsilon}\}^{\mathrm{T}}[C]\left(\{\varepsilon\}-\left\{\varepsilon^{pl}\right\}\right)d\Omega = \left\{\bar{d}\right\}^T\{R\} \tag{37}$$

Substituting relations (16) and (36) into relation (37) the following expression is obtained:

$$\begin{aligned}&\left\{\bar{d}\right\}^{T}\int_{\Omega}\left[B\right]^{\mathrm{T}}\left[C\right]\left(\left[B\right]\left\{d\right\}-\left[\tilde{N}^{pl}\right]\left\{z\right\}\right)d\Omega=\left\{\bar{d}\right\}^{T}\left\{R\right\}\Leftrightarrow\\&\int_{\Omega}\left[B\right]^{\mathrm{T}}\left[C\right]\left[B\right]\left\{d\right\}d\Omega-\int_{\Omega}\left[B\right]^{\mathrm{T}}\left[C\right]\left[\tilde{N}^{pl}\right]\left\{z\right\}d\Omega=\left\{R\right\}\end{aligned}\tag{38}$$

and finally the following constitutive equation is deduced at the patch level:

$$\left[k_e\right]\left\{d\right\}-\left[k_h\right]\left\{z\right\}=\left[\underset{((2\times n\times m)\times(2\times n\times m))}{\left[k_e\right]}\;\vdots\;\underset{((2\times n\times m)\times(3\times nPl\times mPl))}{-\left[k_h\right]}\right]\left\{\begin{matrix}\left\{d\right\}\\\hline\left\{z\right\}\end{matrix}\right\}=\left\{R\right\}\tag{39}$$

where $\left[k_e\right]$ is the isogeometric elastic and $\left[k_h\right]$ the herein introduced hysteretic stiffness matrix.

The unknown vector $\left\{z\right\}$, containing all plastic strains at quadrature points follows an evolutionary equation of Bouc-Wen type given in relation (33) independently for every three component plastic strain vector. It becomes evident that the proposed formulation can be used also for other types of elements in an effort to incorporate directly the hysteretic behavior.

6 STATE EQUATIONS - SOLUTION PROCEDURE

The equation of motion is expressed as:

$$\left[m\right]\left\{\ddot{d}\right\}+\left[c\right]\left\{\dot{d}\right\}+\left[k_e\right]\left\{d\right\}-\left[k_h\right]\left\{z\right\}=\left\{R(t)\right\}\tag{40}$$

In addition to the linear equations of motion (Eq. (40)), the uncoupled non-linear evolution equations of the hysteretic degrees of freedom (Eq. (33)) for each quadrature point are required. The system of differential equations of motion and evolution equations can be transformed into state space form introducing further the nodal velocities as additional unknowns:

$$\begin{aligned}&\left\{\dot{X}_1\right\}=\left\{X_2\right\}\\&\left\{\dot{X}_2\right\}=-\left[m\right]^{-1}\left(\left[c\right]\left\{X_2\right\}+\left[k_e\right]\left\{X_1\right\}-\left[k_h\right]\left\{X_3\right\}-\left\{P(t)\right\}\right)\\&\left\{\dot{X}_3\right\}=f\left(\left\{X_1\right\},\left\{X_2\right\},\left\{X_3\right\}\right)\end{aligned}\tag{41}$$

where $\left\{X_1\right\}$ is the vector of unknown displacements, $\left\{X_2\right\}$ the corresponding vector of unknown velocities and $\left\{X_3\right\}$ the vector of the hysteretic degrees of freedom. The system of Eq. (41) suffices to determine the nonlinear dynamic behavior of the structure. The system of first order nonlinear differential equations can be solved using Runge – Kutta predictor-corrector type of integrator schemes, such as the Livermore family of solvers (Radhakrishnan and Hindmarsh 1993), allowing for robust and unconditionally stable solutions.

A basic advantage of the proposed method is that the load is handled through the system of first order differential equations. Thus the method accounts for the inherent inelasticity i.e., the flow rule and consistency condition after yielding and the correction is strictly numerical to achieve the desired accuracy, whereas in a radial return scheme the predictor step is linear and all inelastic considerations are in the corrector step.

Using the proposed element, shape optimization of elastic problems can be easily formulated by selecting the coordinates and/or weights of the control points of the NURBS geometry as design variables aiming at minimizing the mass of the structure under specific loading and a set of stress and/or displacement constraints imposed at specific points [5].

7 NUMERICAL EXAMPLES

1st example

An Isogeometric Analysis code was developed to implement the proposed formulation. In this example, the optimization of a simply supported beam with a predefined length of $l=8m$ is initially examined. An elastoplastic material is considered with $E=210GPa$, $\nu=0.3$, $\sigma_y=235MPa$, $E_t=21GPa$ and thickness $t=0.08m$. In addition, the material follows the von – Mises yield criterion with linear kinematic hardening law. The objective is to minimize the weight of the beam loaded by a concentrated force $P=1000kN$ at the

midpoint, subjected to two non-linear constraints, the first of which requires that the deflection at the midpoint of the beam $u_{mid} \le 0.01m$ and the second demands that the von Mises stress at the extreme bottom fiber of the midpoint $\sigma_{VM} \le \sigma_y$. The initial shape of the beam is a rectangle of height $h = 2m$. The biquadratic ($p = 2$, $q = 2$) NURBS surface is formed from knot vectors $\Xi = \mathrm{H} = \{0, 0, 0, 0.5, 0.5, 1, 1, 1\}$ and the control weights are defined $w_{i,j} = 1$ (the NURBS degenerates to B-spline surface). The optimization variables are the vertical positions of control points of the bottom row, the vertical positions of control points of the upper row, which are constrained to lie on a straight horizontal line, whereas the intermediate points are linked to the extreme points. The optimization problem is solved using the fmincon solver of MATLAB which is appropriate for the minimization of constrained nonlinear multivariable functions. The initial and the optimized shape of the beam are shown in Figure 2.

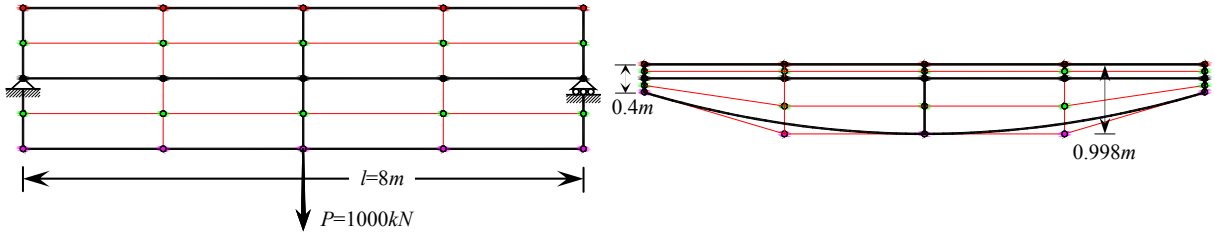

Figure 2. Initial and the optimized shape of the beam

Subsequently, the optimized beam is refined by inserting new knots and raising the polynomial order of the basis functions. The structure is subjected to monotonically increasing concentrated load $P = 5000kN$ at the midpoint, which leads to gradual yielding of the beam. In Figure 3, the applied load is plotted against the vertical deflection of the midpoint. The load-deflection curve is compared with the one obtained using Abaqus.

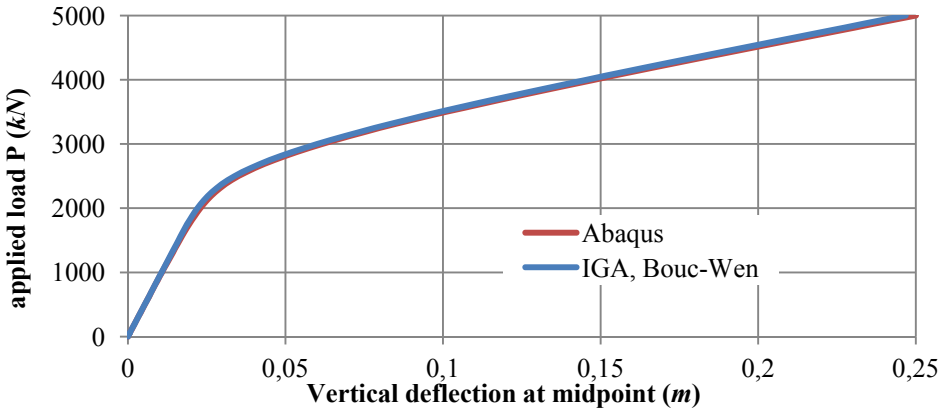

Figure 3. Load-deflection curve at midpoint of the beam

From the previous curve, it is apparent that the solution obtained based on the Bouc-Wen hysteretic model implemented in an IGA code agrees well with the solution obtained using Abaqus. Finally, the distribution of the von-Mises stress of the beam is illustrated in Figure 4.

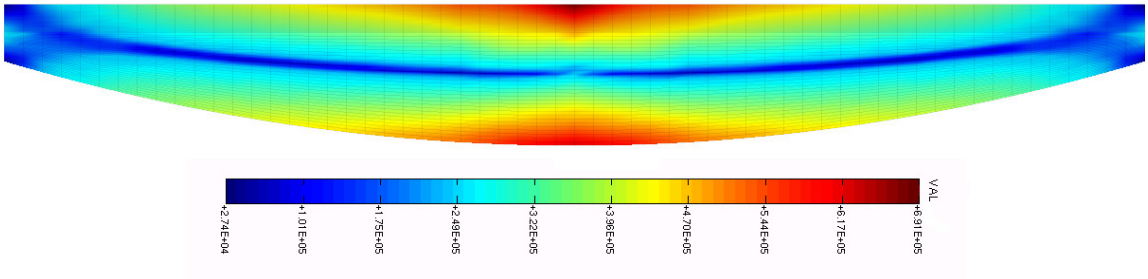

Figure 4. Distribution of the von-Mises stress (kN/m^2)

2nd example

In the 2nd example, the optimum outer shape of an open spanner-wrench with a predefined length of

$l = 25cm$ is investigated. An elastoplastic material is considered with $E = 210GPa$, $\nu = 0.3$, $\sigma_y = 235MPa$, $E_t = 21GPa$ and thickness $t = 1cm$. In addition, the material follows the von – Mises yield criterion with linear kinematic hardening. The objective is to minimize the weight of the spanner loaded by a concentrated force $P = 1kN$ at point A (Figure 5), subjected to a non-linear constraint requiring that the deflection at point A $u_A \leq 0.1cm$. The optimization variables are the vertical positions of control points of the bottom row, the upper row is symmetric to the bottom one, whereas the intermediate points are linked to the extreme points. Moreover, an additional constraint aligns the control points of the handle. The optimization problem is solved by fmincon solver of MATLAB. The optimized shape of the spanner is shown in Figure 5.

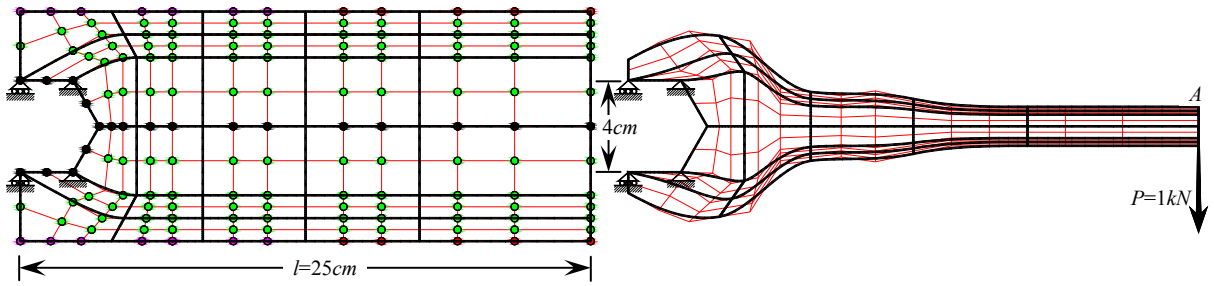

Figure 5. Initial and the optimized shape of the open spanner

The performance of the optimization algorithm is depicted in Figure 6.

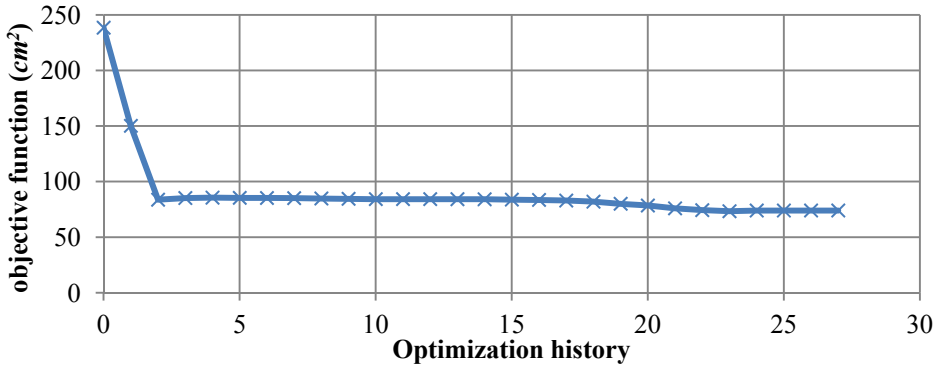

Figure 6. Evolution of the optimization procedure

Subsequently, the optimized spanner is subjected to monotonically increasing concentrated load $P = 4kN$ at point A, in excess of its nominal value, which leads to gradual yielding. In Figure 7, the applied load is plotted against the vertical deflection at point A. The load-deflection curve is compared with the one obtained using Abaqus.

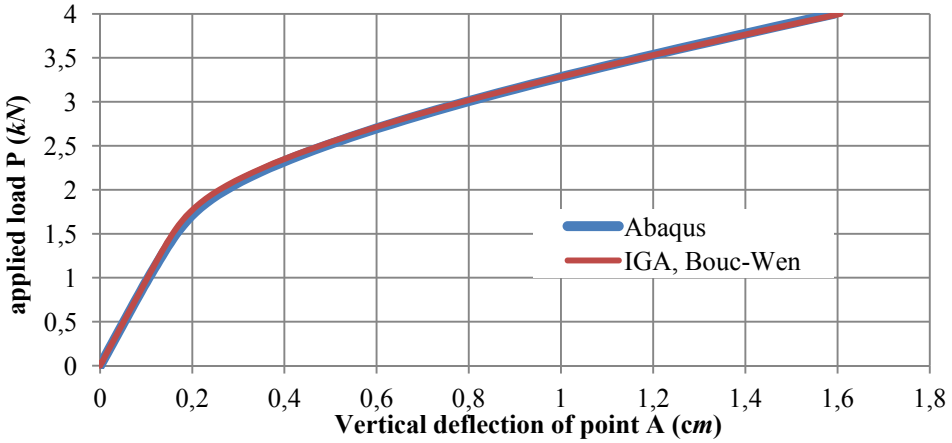

Figure 7. Load-deflection curve of the point A of the spanner

Finally, the distribution of stress component σ_{xx} of the spanner is illustrated in Figure 8.

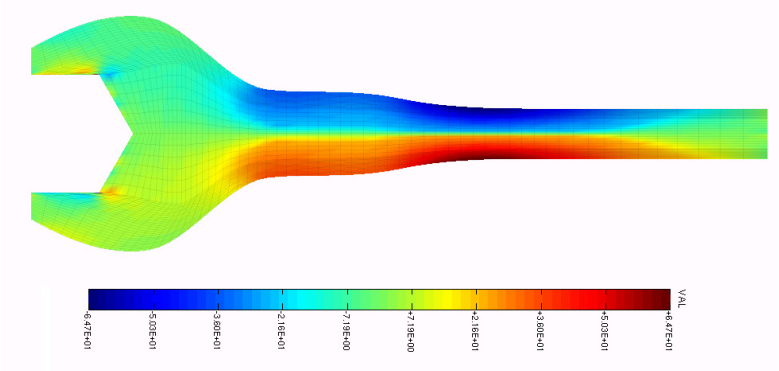

Figure 8. Stress component σ_{xx} (kN/cm^2)

8 CONCLUSIONS

A new hysteretic formulation for the inelastic static and dynamic analysis of plane stress problems within the framework of Isogeometric Analysis (IGA) is presented. One of the advantages of the proposed method relies on the fact that the response is handled through the system of first order differential equations. This provides the displacements at control points, the elastic and plastic strains and the stresses at quadrature points that satisfy the inelastic constitutive relations and equilibrium without any additional iterative process. Therefore, by solving the system of differential equations numerically, the scheme stays always on the yield function and satisfies the flow rule by definition. Consequently, the local iterations of Newton – Raphson method are avoided, at the expense of the numerical solution of first order evolution equations for the introduced additional hysteretic unknowns. Moreover, the proposed formulation utilizes the inelastic constitutive relation in the principle of virtual work in a separable form distinguishing the elastic and hysteretic part. The derived structural matrices are evaluated only once, at the beginning of the analysis procedure. Thus, the proposed formulation directly accounts for inelasticity in a natural way by solving in coupled form the linear equilibrium equations together with the non-linear evolution equations, avoiding the trial elastic predictions followed by plastic corrections. Finally, the proposed method avoids the tedious evaluation of the nodal internal forces of standard methods employing numerical integration over the element volume in every inner step. For these reasons, the proposed formulation turns out computationally more efficient for the same accuracy as compared to standard methods. The IGA formulation through the control points and their weights is proved more efficient for shape optimization problems as compared to the standard isoparametric formulation.

REFERENCES

[1] Piegl, L., Tiller, W. (1996), *The NURBS Book(Monographs in Visual Communication)*, Springer Berlin Heidelberg

[2] T.J.R. Hughes, J.A. Cottrell and Y. Bazilevs, “Isogeometric analysis: CAD, finite elements, NURBS, exact geometry and mesh refinement”, *Computer Methods in Applied Mechanics and Engineering*, 194 (39-41), pp. 4135-4195, (2005).

[3] Triantafyllou, S. P., and Koumousis, V. K. (2012). “A hysteretic quadrilateral plane stress element.” *Arch. Appl. Mech.*, 82(10–11), 1675–1687.

[4] Triantafyllou, S. P., and Koumousis, V. K. (2014). “Hysteretic finite elements for nonlinear static and dynamic analysis of structures.” *J. Eng. Mech.*, 10.1061/(ASCE) EM.1943-7889.0000699, 04014025.

[5] Wolfgang A. Wall, Moritz A. Frenzel, Christian Cyron, “Isogeometric structural shape optimization”, *Computer Methods in Applied Mechanics and Engineering*, 197 (33-40), (2008).